Basin Research (2006) **18**, 375–391, doi: 10.1111/j.1365-2117.2006.00307.x

Tectonic evolution of the Himalaya constrained by detrital ^{40}Ar–^{39}Ar, Sm–Nd and petrographic data from the Siwalik foreland basin succession, SW Nepal

A. G. Szulc,* Y. Najman,† H. D. Sinclair,* M. Pringle,‡ M. Bickle,§ H. Chapman,§ E. Garzanti,¶ S. Andò,¶ P. Huyghe,‖ J-L. Mugnier,‖ T. Ojha** and P. DeCelles†

*School of GeoScience, University of Edinburgh, Edinburgh, UK
†Department of Environmental Science, University of Lancaster, Lancaster, UK
‡Earth, Atmospheric and Planetary Sciences, Massachusetts Institute of Technology, Cambridge, Massachusetts, MA, USA
§Department of Earth Sciences, University of Cambridge, Cambridge, UK
¶Dipartimento di Scienze Geologiche e Geotecnologie, Università di Milano-Bicocca, Milan, Italy
‖Laboratoire de Géodynamique des Chaînes Alpines, Université Joseph Fourier, Grenoble, France
**Himalayan Experience, Mhepi, Kathmandu, Nepal
†Department of Geosciences, University of Arizona, Tucson, AZ, USA

ABSTRACT

^{40}Ar–^{39}Ar dating of detrital white micas, petrography and heavy mineral analysis and whole-rock geochemistry has been applied to three time-equivalent sections through the Siwalik Group molasse in SW Nepal [Tinau Khola section (12–6 Ma), Surai Khola section (12–1 Ma) and Karnali section (16–5 Ma)]. ^{40}Ar–^{39}Ar ages from 1415 single detrital white micas show a peak of ages between 20 and 15 Ma for all the three sections, corresponding to the period of most extensive exhumation of the Greater Himalaya. Lag times of less than 5 Myr persist until 10 Ma, indicating Greater Himalayan exhumation rates of up to 2.6 mm year^{-1}, using one-dimensional thermal modelling. There are few micas younger than 12 Ma, no lag times of less than 6 Myr after 10 Ma and whole-rock geochemistry and petrography show a significant provenance change at 12 Ma indicating erosion from the Lesser Himalaya at this time. These changes suggest a switch in the dynamics of the orogen that took place during the 12–10 Ma period whereby most strain began to be accommodated by structures within the Lesser Himalaya as opposed to the Greater Himalaya. Consistent data from all three Siwalik sections suggest a lateral continuity in tectonic evolution for the central Himalayas.

INTRODUCTION

Growth of the Himalayas and the Tibetan Plateau is held responsible for major changes in the Late Cretaceous and Cenozoic climate and seawater chemistry (Prell & Kutzbach, 1992; Raymo & Ruddiman, 1992; Harrison *et al.*, 1993; Quade *et al.*, 1995, 1997; Dettman *et al.*, 2001). Various models have been proposed for the tectonic evolution of this region, yet the processes that have controlled crustal deformation and exhumation are much debated (e.g. Coward & Butler, 1985; Searle, 1991; Schelling, 1992; Ratschbacher *et al.*, 1994; Srivastava & Mitra, 1994; Hauck *et al.*, 1998; Hodges, 2000; Beaumont *et al.*, 2001; DeCelles *et al.*, 2001; Tapponnier *et al.*, 2001; Robinson *et al.*, 2003, 2006).

The metamorphic core of the orogen (Greater Himalayan zone) was exhumed between the Main Central Thrust and South Tibetan Detachment fault systems (Burchfiel *et al.*, 1992; Hodges *et al.*, 1992; Vannay & Hodges, 1996; Fig. 1). Although isotopic data suggest that most Greater Himalayan exhumation occurred between ~23 and 16 Ma and the slab had cooled below the Ar closure temperature for muscovite by ~15 Ma, the timing of cessation of exhumation or whether or not movement has continued, perhaps episodically until the present, is unclear (Burg & Chen, 1984; Hubbard & Harrison, 1989; Harrison *et al.*, 1992; Coleman, 1996; Hodges *et al.*, 1996; Vannay & Hodges, 1996; Coleman & Hodges, 1998; Walker *et al.*, 1999; Stephenson *et al.*, 2000; Godin *et al.*, 2001; Daniel *et al.*, 2003; Searle & Godin, 2003; Searle *et al.*, 2003). A number of younger (Late Miocene–Pliocene) Th–Pb monazite ages have been found in proximity to the Main Central Thrust within Greater Himalayan and (mostly) Lesser Himalayan lithologies (Fig. 1). The young ages have been interpreted by some as a separate pulse of the Main Central Thrust reactivation at ~8–6 Ma and imply >20 km of exhumation since then (Harrison *et al.*, 1997; Catlos *et al.*, 2001, 2002). However, other authors suggest that these young mineral

Correspondence: A. G. Szulc, School of GeoScience, University of Edinburgh, West Mains Road, Edinburgh EH9 3JW, UK. E-mail: Adam.Szulc@glg.ed.ac.uk

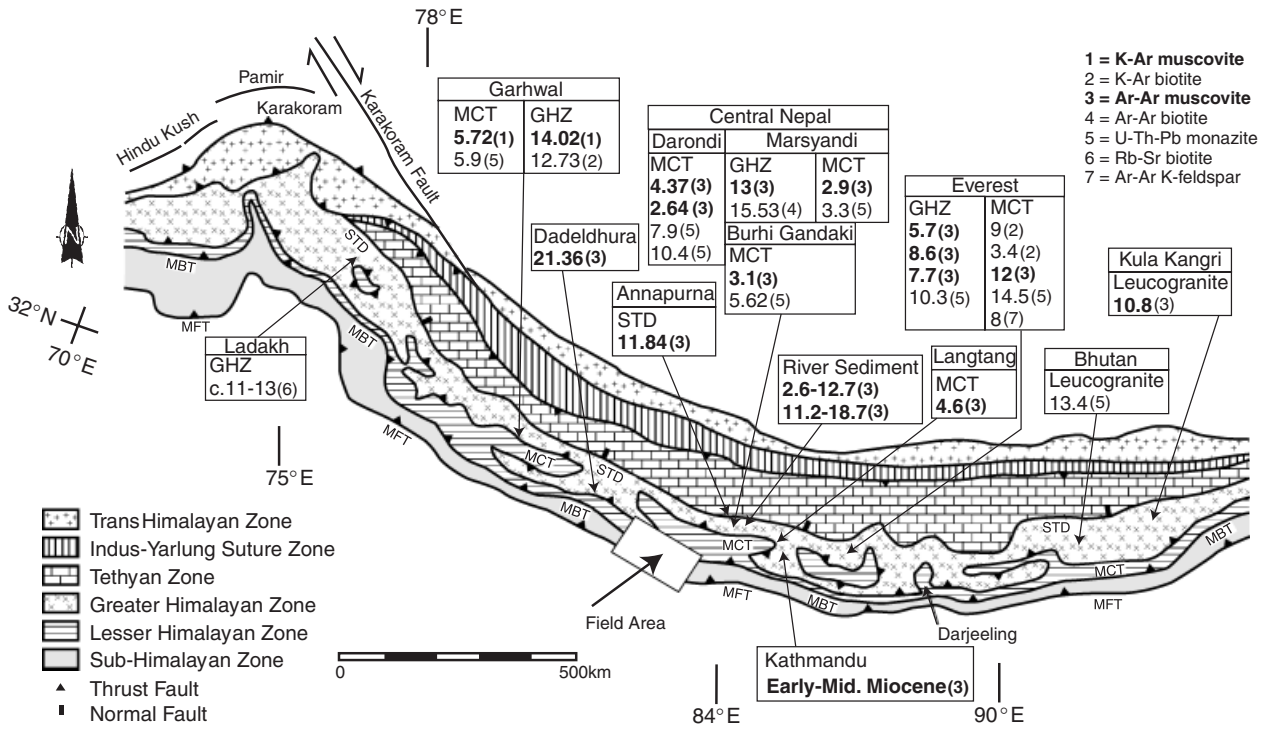

Fig. 1. Geological map of the Himalaya, adapted from Searle *et al.* (2003), showing young age data as evidence for most recent tectonics. Relevant dating technique is shown in key. Only the Siwalik Group north of the Indian border is shown. Data sources: Ladakh (Honegger *et al.*, 1982), Garhwal (Metcalf, 1993; Catlos *et al.*, 2002), Dadeldhura (DeCelles *et al.*, 2001), Annapurna (Godin *et al.*, 2001), Central Nepal (Copeland *et al.*, 1991; Edwards, 1995; Vannay & Hodges, 1996; Harrison *et al.*, 1997; Coleman & Hodges, 1998; Catlos *et al.*, 2001; Kohn *et al.*, 2001), river sediment (Brewer *et al.*, 2003), Langtang (Macfarlane, 1993), Kathmandu (Copeland *et al.*, 1996), Everest (Catlos *et al.*, 2002), Bhutan (Daniel *et al.*, 2003), Kula Kangri (Maluski *et al.*, 1988). GHZ, Greater Himalayan Zone; STD, South Tibetan Detachment; MCT, Main Central Thrust; MBT, Main Boundary Thrust; MFT, Main Frontal Thrust.

ages may be the result of resetting by hydrothermal activity rather than due to tectonics (e.g. Searle *et al.*, 2002; Bollinger & Janots, 2006). Exhumation of Lesser Himalayan units above a duplex in the footwall of the Main Central Thrust is thought to have followed the main phase of the Greater Himalayan activity (~12–5 Ma; DeCelles *et al.*, 1998a, 2001; Bollinger *et al.*, 2004; Robinson *et al.*, 2006). The exact nature and timing of duplex development is also uncertain, mainly owing to poor exposure and a lack of suitable datable minerals in the Lesser Himalaya.

In this paper, we use the detrital record of the Himalayan foreland basin to investigate orogenic development during the Neogene. Foreland basin sediments are analysed using detrital mineral ages with the purpose of testing tectonic, geomorphologic and climatic models for the adjacent hinterland (e.g. Dickinson *et al.*, 1983; Allen *et al.*, 1986; Garver *et al.*, 1999; Bernet & Spiegel, 2004). Whereas the mineralogical and isotopic evidence for early stages of orogenesis may be gradually lost in the hinterland through either denudation or overprinting by later stages of metamorphism, much of this record can be preserved in the foreland basin. Being zoned in terms of lithology, age and geochemistry (thus aiding provenance determination; Table 1) and boasting the world's largest terrestrial foreland basin, the Himalayan orogen lends itself to the detrital approach. Such investigations have therefore greatly enhanced our understanding of the Himalayan evolution (e.g. Harrison *et al.*, 1993; Najman *et al.*, 1997; DeCelles *et al.*, 1998b, 2001, 2004; Najman & Garzanti, 2000; Huyghe *et al.*, 2001; White *et al.*, 2002). Along the deformation front, the Sub-Himalayan Zone of Nepal comprises imbricated thrust sheets of the Siwalik Group molasse, with up to 6 km of continuously exposed sediment that was deposited during the last 16 m.y. (Burbank *et al.*, 1996; Mugnier *et al.*, 1999, 2004; Lavé & Avouac, 2000). We focus on three time-equivalent sections through the Siwalik thrust sheets in SW Nepal, separated by at least the equivalent of the modern transverse drainage spacing [Tinau Khola section (12–6 Ma); Surai Khola section (12–1 Ma) and Karnali section (16–5 Ma), dated by magnetostratigraphy; Gautam & Fujiwara, 2000; Ojha *et al.*, 2000, 2001; Figs 2 and 3]. Use of more than one coeval section, with sufficient lateral spacing, allows us to differentiate between local signals produced by sediment ponding or drainage diversion, and regional tectonic signals that would affect all three sections. This approach therefore regionalises our interpretations and provides a spatial test of the detrital technique.

Alternative magnetostratigraphic ages for the Surai (Appel *et al.*, 1991) and Tinau (Gautam & Appel, 1994) sections are also published. This study uses the age dating of Ojha *et al.* (2001 and unpublished) as their magnetostratigraphic data were collected from laminated siltstones rather than

Table 1. Comparison of lithological, age and geochemical characteristics of the main rock units relevant to this study

	Dominant Lithologies	Age	Geochemistry
Crystalline thrust sheets	Metamorphics up to gnt-grade, granites, sed./low-grade cover	Same as Greater Himalayan Zone	ε_{Nd}: -8 to -12
Greater Himalayan Zone	Medium- to high-grade metamorphics and leucogranites	Proterozoic protolith affected by Himalayan metamorphism. ~40–30 Ma (Eo-Himalayan) ~24–15 Ma (Neo-Himalayan) controversial Late Miocene–Pliocene ages	ε_{Nd}: -5 to -20 $^{87}Sr/^{86}Sr$: 0.73–0.84
Tibetan Himalayan Zone	Sediments, carbonates, and low-grade metasediments	Palaeozoic to Eocene	ε_{Nd}: -6 to -20 $^{87}Sr/^{86}Sr$: 0.7–0.75
GHZ protolith/cover (Haimanta).	Sediments and low-grade metasediments	Late Proterozoic	ε_{Nd}: -8 to -19 $^{87}Sr/^{86}Sr$: 0.7–0.75
Lesser Himalayan Zone	Sediments, low-grade metasediments and carbonates, volcanic and granitic components	Palaeoproterozoic to Tertiary	ε_{Nd}: Inner LHZ: -19 to -28 Outer LHZ: -11 to -18 $^{87}Sr/^{86}Sr$: mostly > 0.8

Data sources – Tibetan Himalayan Zone: Schneider & Masch (1993), Derry & France-Lanord (1996), Harrison *et al.* (1997), Garzanti (1999), Godin *et al.* (1999), Najman *et al.* (2000); Greater Himalayan Zone: Treloar & Rex (1990), Vannay & Hodges (1996), Vance & Harris (1999), Najman *et al.* (2000), Searle *et al.* (2003); Greater Himalayan Zone protoliths: Parrish & Hodges (1996), Richards *et al.* (2005); Lesser Himalayan Zone: Valdiya (1980), Sakai (1983), Ahmad *et al.* (2000), Najman *et al.* (2000); Crystalline Thrust Sheets: DeCelles *et al.* (2001), Robinson *et al.* (2001). ε_{Nd} calculated for $t = 0$.

sandstones. Finer-grained facies generally provide more reliable magnetic age data due to the greater abundance of single magnetic domain particles (Butler, 1992). However, the difference does not have significant effect on our final interpretations, since over the crucial 12–10 Ma period, the ages show reasonable correlation (Fig. 4).

The results of ^{40}Ar–^{39}Ar dating of single detrital white micas are presented, which, when compared with the depositional age of the host sediment, provides information about source-area exhumation rates (e.g. Copeland & Harrison, 1990). This is combined with petrography and heavy mineral analyses and whole-rock Nd and Sr isotope geochemistry to further constrain the provenance of the sediment under scrutiny. Analyses were performed on samples taken at 1 m.y. intervals along each section.

TECTONIC SETTING

At ~52 Ma the northern margin of the Indian continental plate collided with the Andean-type southern margin of Eurasia (Garzanti *et al.*, 1987, 1996; Klootwijk *et al.*, 1992; DeCelles *et al.*, 2004). Following closure of the Tethys Ocean and subduction of the Indian plate, orogenesis involved the accretion of the Indian plate material and southward progression of thrusting and exhumation relative to Eurasia, accommodating hundreds of kilometres of shortening (Dewey *et al.*, 1989; Hodges, 2000; Johnson, 2003; Murphy & Yin, 2003; Robinson *et al.*, 2006).

Lithotectonic zones

The Himalayas are divided into a series of lithotectonic zones (Fig. 1) with distinct isotopic and petrographic characteristics (Table 1). Starting in the north, the site of collision is marked by the Indus–Yarlung Suture zone, comprising ophiolites and flysch material (Searle, 1983; Garzanti & Van Haver, 1988). These rocks were thrust southwards onto the north Indian passive continental margin, represented by Palaeozoic to Eocene sediments of the Tibetan Himalayan Zone/Tethyan Himalaya (Gaetani & Garzanti, 1991; Garzanti, 1999). A series of north-dipping normal faults, collectively known as the South Tibetan Detachment system, separates the Tibetan Himalayan Zone (hanging wall) from the Greater Himalayan Zone (foot wall). Crustal thickening following on from India–Asia collision culminated in Barrovian metamorphism (~8–10 kbar, 550–700 °C) between ~40 and 30 Ma (Treloar & Rex, 1990; Vance & Harris, 1999; Simpson *et al.*, 2000), as recorded in the medium–high grade metamorphosed rocks of the Greater Himalaya. This was followed by decompression and isobaric cooling from ~22 Ma. High Himalayan protolith or cover, such as the Haimanta and Sanctuary Formations, which perhaps graded up into the Tethyan Himalaya, escaped Cenozoic metamorphism (Colchen *et al.*, 1986; Pognante *et al.*, 1990; Thakur 1998).

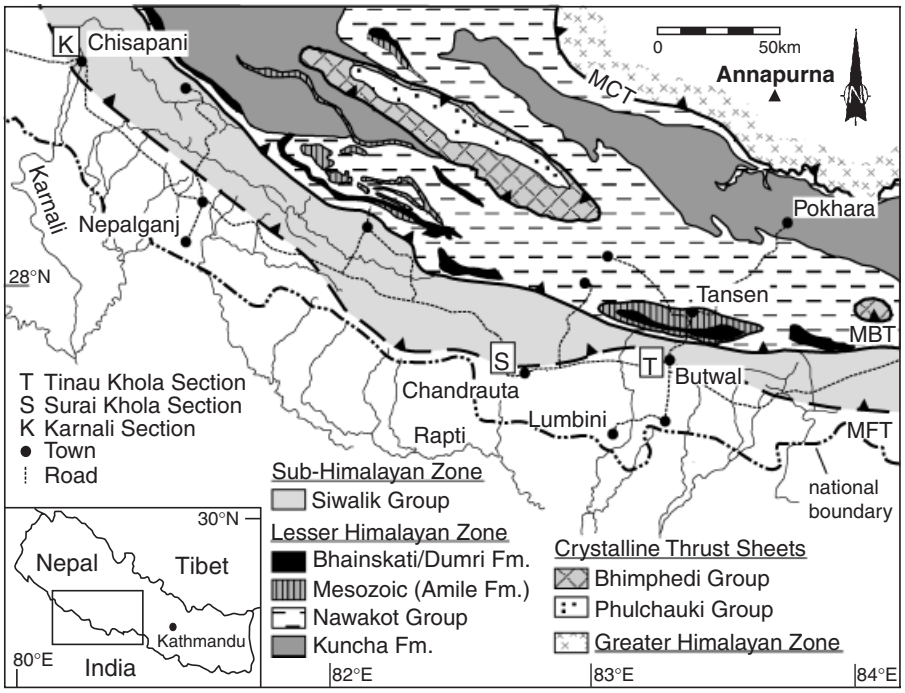

Fig. 2. Geological map of SW Nepal, inset shows map location. Locations of the three sections under investigation are highlighted. MCT, Main Central Thrust, MBT, Main Boundary Thrust, MFT, Main Frontal Thrust. Modified from Amatya & Jnawali (1994).

Outcrops are preserved both south and north of the Main Central Thrust, which separates the Greater Himalaya in the hanging wall from the Lesser Himalaya in the footwall. The South Tibetan Detachment System, together with the Main Central Thrust facilitated the Greater Himalayan exhumation.

Metamorphism of low-grade Lesser Himalayan rocks occurred before Himalayan orogenesis and was followed by Himalayan diagenetic to localised garnet grade metamorphism (Paudel & Arita, 2000). In India, the Lesser Himalaya are divided into the Inner and Outer zones (Valdiya, 1995), which yield distinct Nd isotope signatures. This isotopic distinction has not yet been applied in western Nepal (Valdiya 1995; Ahmad *et al*., 2000; Robinson *et al*., 2001; Richards *et al*., 2005; Table 1). Overlying the Lesser Himalaya, a series of synformal Crystalline Thrust Sheets have similarities to Greater Himalayan rocks and were emplaced between 22 and 14 Ma, contemporaneous with the Main Central Thrust (Valdiya, 1980; Copeland *et al*., 1996; Upreti & Le Fort, 1999; DeCelles *et al*., 2001; Fig. 1). Eocene–Miocene foreland basin deposits (Bhainskati and Dumri Formations) also occur above the Lesser Himalayan units in Nepal (Sakai, 1983; DeCelles *et al*., 1998a, 2004). Lesser Himalayan rocks were thrust southwards over the Sub-Himalayan Zone along the Main Boundary Thrust probably at some point within the last 12 m.y. (Meigs *et al*., 1995; Burbank *et al*., 1996; DeCelles *et al*., 1998a, 2001; Najman *et al*., 2004). More recent movement has carried the Sub-Himalaya above Quaternary deposits of the modern foreland along the Main Frontal Thrust, the locus of most current Himalayan shortening (Mugnier *et al*., 1993; Lavé & Avouac, 2000).

SIWALIK STRATIGRAPHY

The Siwalik Group molasse in Nepal consists of 4–6 km of Mid-Miocene to Pliocene fluvially deposited sediments (Parkash *et al*., 1980; Burbank *et al*., 1996). Following the creation of significant topography, detritus feeding the Himalayan foreland basin has been derived mostly from the southern slope of the Himalayas (France-Lanord *et al*., 1993; Garzanti *et al*., 1996). Consequently, the Siwalik Group comprises detritus from Greater Himalayan, Lesser Himalayan and Tibetan Himalayan source areas. Figure 3 shows simplified logs for the three sections analysed, which are comparable with Siwalik descriptions along the length of the Himalayas (Parkash *et al*., 1980; Harrison *et al*., 1993; Willis, 1993; Quade *et al*., 1995; Burbank *et al*., 1996; DeCelles *et al*., 1998a; Nakayama & Ulak, 1999). In general, the Siwalik Group can be described as a coarsening – (grain size: 100–450 m) and thickening – (beds: few centimetres to >5 m) upwards succession of mudstone and sandstone with conglomerate in the upper part. Conglomerate has been removed by faulting along the Tinau Khola section and is present along the Karnali section but occurs above the level of youngest magnetostratigraphic dating at $\sim$5 Ma (Gautam & Fujiwara, 2000). The older, finer-grained deposits consist of floodplain, palaeosol, crevasse splay and small channel facies. These are superseded up-section in turn by the meandering channel and eventually conglomeratic braided river facies in the uppermost Siwalik units.

A total of 2440 palaeocurrent directions were measured from trough- and planar-cross lamination, flutes, ripples, channels, imbrication, parting lineation, grooves and tool

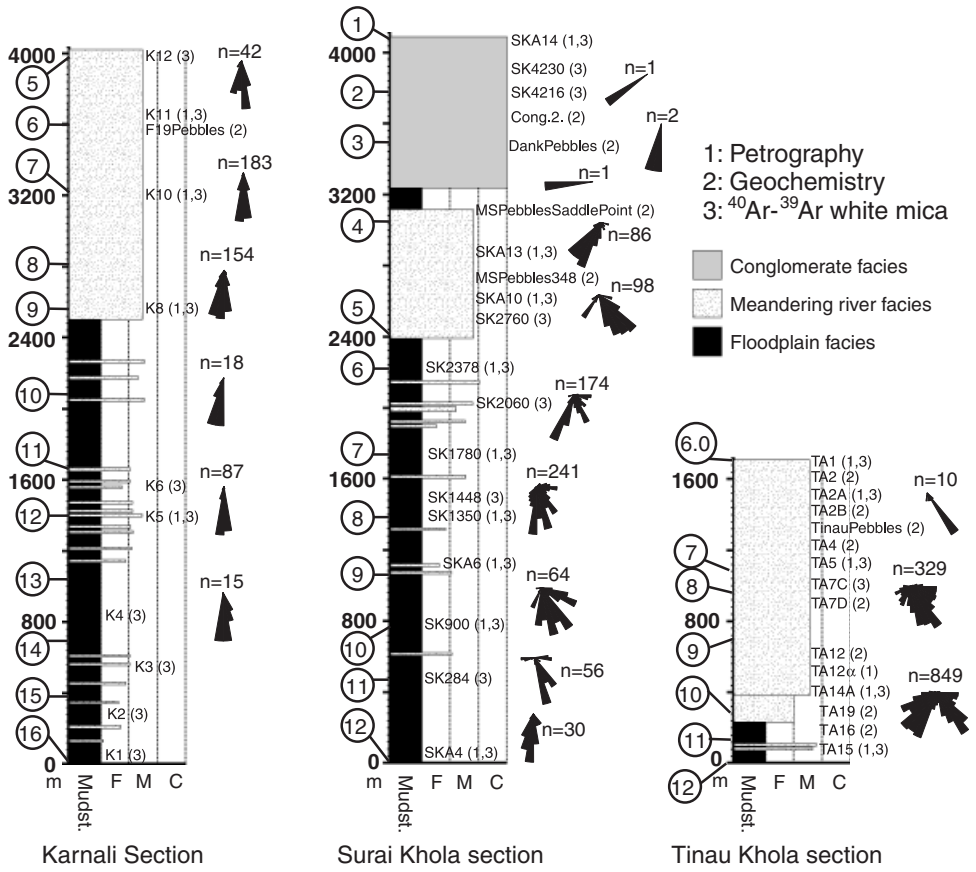

Fig. 3. Simplified logs for the three Siwalik Group sections used in this study. Magnetostratigraphic ages are shown in circles. The magnetic data are from Gautam & Fujiwara (2000) (Karnali) and T. P. Ojha et al. (unpublished; Tinau Khola and Surai Khola) and ages are based on the geomagnetic timescale of Cande & Kent (1995). Sample locations are shown with types of analyses in brackets. The Tinau Khola and Surai Khola sections are incomplete due to thrusting; the top of the Karnali section was not accessible at the time of research. Samples K15 (1), K13 (3) and K13Pebbles (2) taken from the Karnali section are not indicated because they were sampled above the top of the log which ends with the youngest available magnetostratigraphic age. The ages for these samples were thus inferred from their stratigraphic position. Palaeoflow rosettes group data into 400 m intervals (measurements from trough- and planar-cross lamination, flutes, ripples, channels, imbrication, parting lineation, grooves and tools).

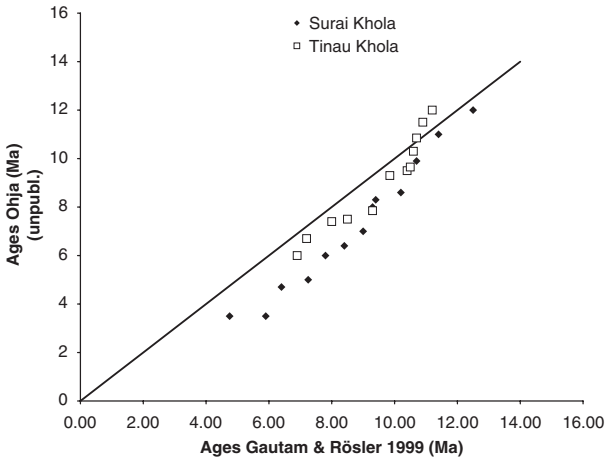

Fig. 4. Comparison of palaeomagnetic ages for T. P. Ojha et al. (unpublished and 2001) vs. Appel *et al.* (1991) / Gautam & Appel (1994) for the Tinau Khola and Surai Khola sections. Ages are based on the geomagnetic timescale of Cande & Kent (1995), the Appel *et al.* (1991) and Gautam & Appel (1994) ages were taken from Gautam & Rosler (1999).

marks (Fig. 3). These reveal a broadly consistent southward flow, suggesting that the rivers that deposited the sediment were dominantly transverse to the mountain belt. All three sections lack evidence for sustained axial flow (towards WNW or ESE). Our palaeoflow data, and the fact that the Indus–Ganges drainage divide had probably developed by ~15 Ma (DeCelles *et al.*, 1998b) indicate that potential source areas for the Siwalik sections studied can be confined to the Ganges drainage basin. Therefore, the Siwalik sediment of SW Nepal could have been derived from a region extending from NW India to central Nepal. Palaeoflow indicators suggest most sediment had a northern (Nepal) source area.

METHODS

Petrography and heavy minerals

Three hundred points by the Gazzi–Dickinson point-counting method (Ingersoll *et al.*, 1984; Zuffa, 1985), and 200–250 transparent heavy minerals by the 'ribbon-counting' or

'Flett' methods (Manage & Maurer, 1992), were counted on samples from each section at 1 m.y. intervals. Dense minerals were concentrated with sodium metatungstate (density 2.9 g cm^{-3}), using the 63–250 μm size fraction treated with oxalic and acetic acid to eliminate iron oxides, and carbonates, respectively (Parfenoff *et al*., 1970). Metamorphic lithic grains were classified according to both composition and metamorphic grade, mainly inferred from the degree of recrystallisation of mica flakes (Garzanti & Vezzoli, 2003). Confidence intervals for mean values were calculated according to the Weltje (2002) methods, devised specifically for unitsum constrained data (Aitchison, 1986). Grain-size control was minimised by using only the fine sand fraction for all studied samples. All petrographic work was conducted at the Milano-Bicocca University, Italy.

Whole-rock Sr–Nd geochemistry

Eight whole-rock mudstone and six quartzite pebble samples from sandstones of the Tinau Khola and Surai Khola sections were analysed for Sm–Nd and Rb–Sr isotopic ratios at Cambridge University, England. Analytical techniques follow Ahmad *et al*'s (2000) technique using a mixed ^{150}Nd–^{149}Sm spike. The samples were heated for 8 h at 900 °C to remove organic matter. HF, HNO_3 and Hcl dissolution stages were carried out in Teflon Savillex vials in pressure vessels at 180 °C for 8 h. Sr, Nd and Sm were separated using standard ion-exchange columns (Bickle *et al*., 1988). During the time of these analyses, the internal Johnson Matthey standard ^{143}Nd-^{144}Nd = 0.51111 ± 8 (2 σ) and ^{145}Nd/^{144}Nd = 0.348399 ± 7 (2σ) and NBS987 Sr standard ^{87}Sr/^{86}Sr = 0.710259 ± 8 (2σ). Sr, Nd and Sm blanks were less than 0.05% of sample. Goldstein *et al*'s (1984) chondrite normalised value was used for calculating εNd. In addition, four modern river muds from the Tinau and Karnali Rivers were analysed for Sm–Nd at Ecole Nationale Supérieure, Lyon, France. Nd isotope compositions, determined on whole rocks after classical acid digestion and liquid chromatographic separation (Galy *et al*., 1996, and references therein), were measured on a Nu 500. The Rennes Ames standard was run every two samples and samples Nd isotopic ratios were corrected by sample-standard bracketing to the Rennes Ames values recommended by Chauvel & Blichert-Toft (2001; 143/144 = 0.511961). For samples or standards, the typical 2σ precision for a single run was 0.000006. Blank contributions are negligible for the amount of analysed elements.

Laser fusion ^{40}Ar–^{39}Ar dating of white micas

Single grains of white mica (150 to > 425 μm) were handpicked from 36 sandstone samples and collected in Al foil pots. Sixteen single grains from four different samples were analysed using the step-heating technique to test for alteration. Nearly 1400 single grains were analysed by total fusion. The foil pots were irradiated at the in-core, dummy fuel element facility at the 1 MW TRIGA, Oregon State University. Twenty-one samples were irradiated for 7 h ($\mathcal{J}$ = ~0.001) and 15 samples were irradiated for 12 h ($\mathcal{J}$ = ~0.003). The irradiation fluence parameter, $\mathcal{J}$, was monitored with the Taylor Creek rhyolite sanidine at 28.34 Ma, which was dispersed amongst the foil pots sent for irradiation. Analytical techniques and plateau age calculations follow White *et al*. (2002), except that samples were partially degassed before fusion. Uncertainties are quoted at the 2 σ level of analytical precision. Analyses of the Tinau Khola and Surai Khola sections and samples K1–K4 of the Karnali section were conducted at the Scottish Universities Environmental Research Centre (SUERC). All other Karnali section samples were analysed at MIT, USA.

RESULTS

Petrography and heavy minerals

Petrographic modes and heavy mineral trends are displayed as ternary plots in Fig. 5 and in relation to stratigraphic age in Fig. 6. Full data tables are given in the supplementary material. Sandstone samples from all three sections are quartzo-lithic and plot within the 'recycled orogen' field of Dickinson (1985; Fig. 5). There are no significant differences in bulk composition between the three sections or other coeval Siwalik sections of Nepal along the strike (DeCelles *et al*., 1998b). The sandstones are characterised by large amounts of sedimentary (average 33% of detrital grains) to low-grade metasedimentary lithic grains (average 39% of bulk petrography) and minor medium- and high-grade metamorphic material (average 24% of detrital grains combined). There are high quartz/feldspar ratios and low plagioclase/K-feldspar ratios throughout the succession. Quartz grains are dominantly monocrystalline with subordinate polycrystalline types. Recycling of older sandstones is indicated by the occurrence of rounded quartz grains with abraded overgrowths. In the Karnali section, the proportion of dolostone increases from almost 0 to 5% of detrital grains at 12 Ma.

The proportion of low-grade heavy minerals (epidote, zoisite, chloritoid) increases from 0 up to 27% in all three sections by ~7 Ma (Fig. 6j). Detrital micas are minor (usually < 10% of detrital grains) but are most abundant in the Tinau Khola section (up to 22% of detrital grains; Fig. 6h). Heavy mineral suites mostly constitute 1% or less of detrital grains, and ferromagnesian silicates are rare or lacking, suggesting pronounced diagenetic dissolution of mafic minerals in Nepal. The heavy minerals are dominated by garnet (12–73% of heavy transparent minerals) and ultrastables (zircon, tourmaline, rutile; 9–86% of heavy transparent minerals), along with minor staurolite, kyanite and sillimanite. Kyanite and sillimanite are most common in the Surai Khola section. There are also trace amounts of sphene, apatite, brookite and zoisite. Tourmaline dominates the ultrastables. Rounded ultrastable grains are more abundant in the Tinau Khola and Karnali sections. Combined with low heavy-mineral concentrations, this indicates a greater influence of recycling with respect to sandstones of the Surai Khola section.

Metamorphic minerals show an increase in grade upsection (Fig. 6m). In all three sections, ultrastables and garnet

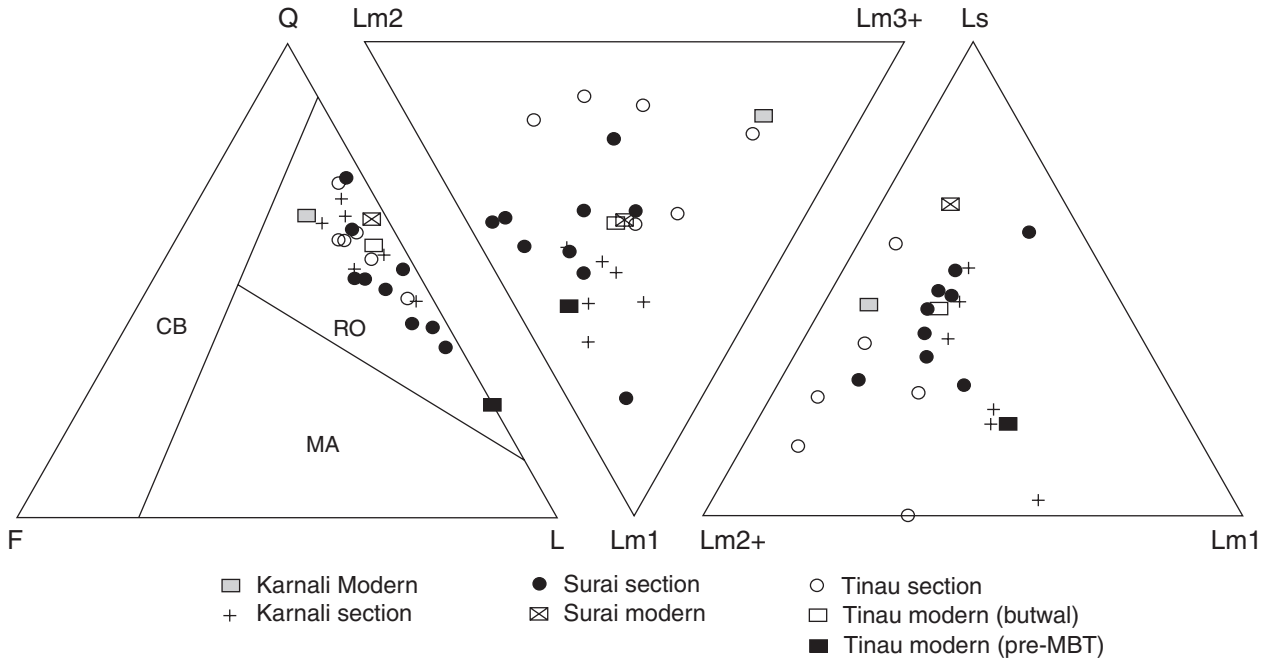

Fig. 5. Petrography ternary plots. Q, quartz; F, feldspars; L, total lithics; Lm1, slate to metasandstone grains; Lm2, phyllite to quartz/sericite grains; Lm2+, Lm2+Lm3+Lm4+Lm5 (low to very high rank, metamorphic lithics with strong cleavage or schistosity); Lm3+, Lm3+Lm4+Lm5 (medium to very high rank, metamorphic lithics with small to large muscovite lamellae); Ls, sedimentary lithics; RO, recycled orogen; MA, magmatic arc; CB, continental block (fields from Dickinson, 1985).

are present from the base of the sections. Staurolite first occurs at 9–10 Ma in both the Karnali and Surai sections, although later at 6 Ma at Tinau. Common kyanite appears in all three sections between 6 and 8 Ma, and it is also at this time that sillimanite appears in the Surai Khola section. The appearance of common kyanite between 8 and 7 Ma coincides with a high feldspar abundance (Fig. 6i) and a high garnet abundance in the Surai Khola section (Fig. 6k). The Tinau Khola and Surai Khola sections also record a slight increase in metamorphic index (MI) during this interval (Fig. 6l).

Whole-rock Sr–Nd geochemistry

Sr and Nd isotopes were measured on 18 samples: seven mudstones and one quartzite clast from the Tinau Khola section, one conglomerate matrix and three quartzite clasts from the Surai Khola section, two quartite clasts from the Karnali section and four modern river muds from the Karnali and Tinau Rivers; data are provided in the supplementary material. Mudstone εNd values are remarkably consistent (Fig. 6e and g). All Tinau Khola mudstone samples and the Surai Khola conglomerate matrix sample yielded εNd values of -17 (Fig. 6e). Figure 7 shows the Siwalik samples compared with average Sr–Nd isotopic values of major Himalayan source zones. Our data for Tinau Khola lies at the overlap of the typical Greater Himalayan Zone and Tibetan Himalayan Zone signatures. The $^{87}Sr/^{86}Sr$ values for Tinau Khola and the Surai Khola conglomerate (Fig. 6g) correlate well with those of previous studies and are very high compared with the global average for rivers of $\sim$0.7119 (Quade *et al.*, 1997). The overlap of geochemical signatures between Himalayan zones complicates provenance determination due to the uncertain effect of sedimentary mixing on the whole-rock detrital geochemistry. Therefore, clasts are a more reliable indicator of provenance for the Siwalik Group. εNd values for the clasts were more varied than the mudstone values, ranging from -14 to -30 (Figs 6f and 7).

^{40}Ar–^{39}Ar dating of single white micas

Step-heating of 16 Surai Khola white micas yielded plateau ages concordant within 95% confidence intervals (MSWD <2.5), which attest to their lack of alteration (Table 2). The ages can therefore be interpreted as geologically meaningful. Although time and cost factors meant that most ages were determined by total fusion (see the supplementary material), the validity of total fusion age data is supported by the step heating results. Figure 8 shows the total fusion ages plotted against stratigraphic age. Figure 6 shows the variation of lag time (defined as the difference between the youngest mica age or youngest peak age and the host sediment depositional age) with stratigraphic age for the youngest mica (Fig. 6a) and youngest peak age (Fig. 6b) from a cumulative probability plot (Fig. 9). The youngest peak age is more reliable for determining lag times because it takes into account the entire white mica population and also the error on the age. Some mica ages from the Karnali section give errors of up to 4 m.y. and two micas plot below the 1 : 1 line (probably due to alteration), good reasons to refer to the youngest peak ages rather than a single grain age. It should be noted that the lag time always

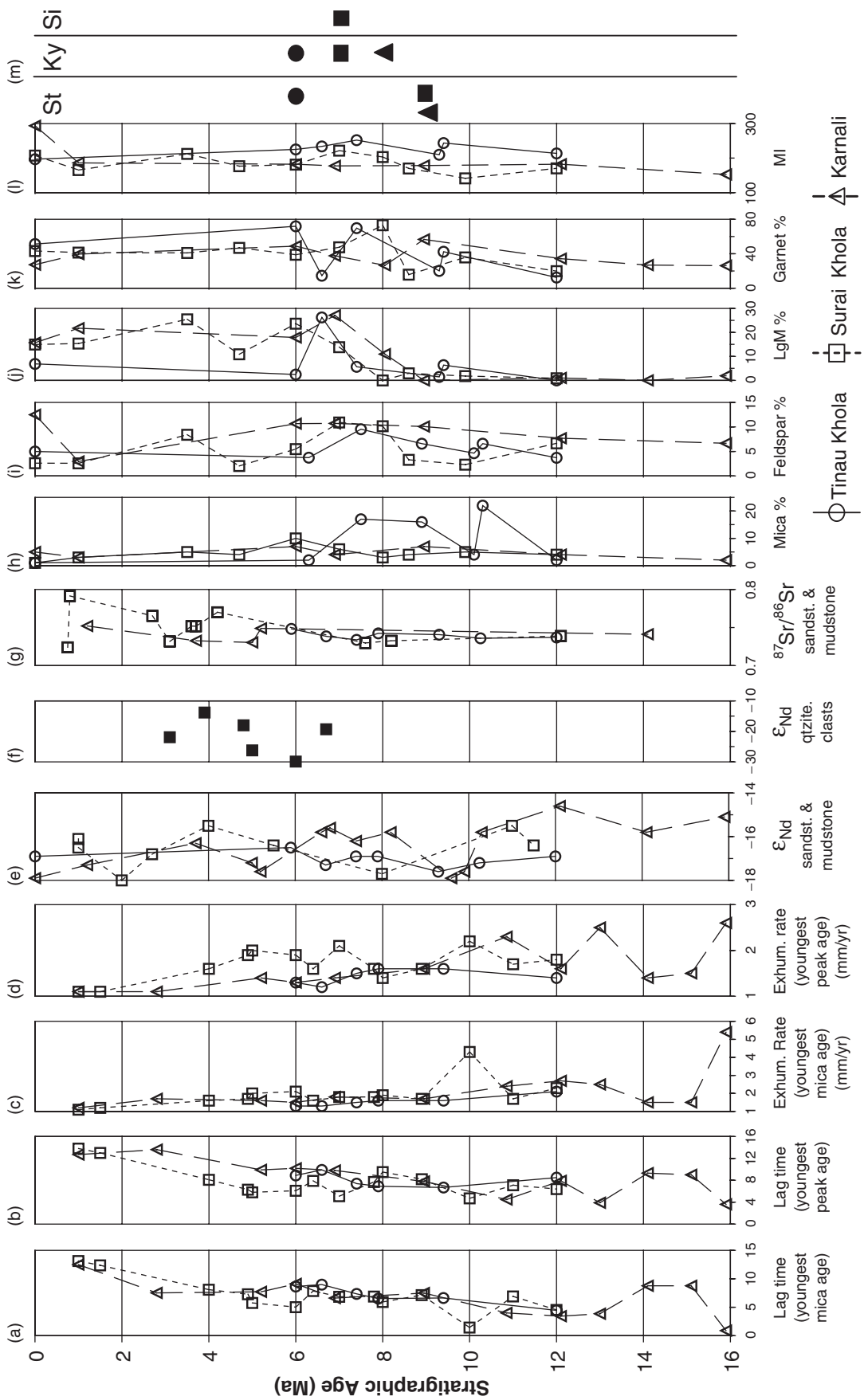

Fig. 6. Variation in detrital signatures with respect to stratigraphic height. Petrographic indices plotted as percentage of detrital component. Circles and solid lines, Tinau Khola; Squares and small dashed lines, Surai Khola; Triangles and long dashed lines, Karnali. (a) and (b) show how the lag time varies depending on whether the youngest single grain age or the youngest peak age is used for the calculation. The youngest Karnali single grain ages that were dated at SURRC were used to calculate lag time for the 16–12 Ma sediment due to the large errors associated with the younger ages that were run at MIT. (c) and (d) show how exhumation rate (using the one dimensional model of White *et al.*, 2002) varies for single grain age and youngest peak age data. (e) includes data from Huyghe *et al.* (2001), Robinson *et al.* (2001) and three unpublished samples from P. Huyghe. (f) gives Nd values for individual quartzite pebbles that are not affected by sedimentary mixing complications. (g) includes data from Galy (1999), Huyghe *et al.* (2001) and two unpublished samples from P. Huyghe. (hk) show petrographic data plotted as a percentage of the detrital component, LgM, low-grade heavy minerals (epidote, zoisite, chloritoid). (l) displays MI or metamorphic index data, see data repository for explanation of MI. (m) indicates when metamorphic index minerals first appear in the section.

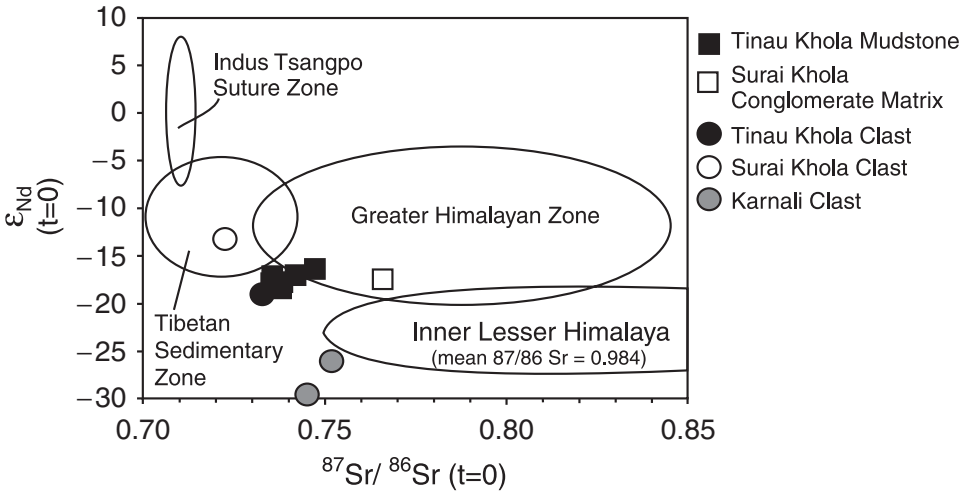

Fig. 7. Whole-rock Nd–Sr isotopic data from the Tinau Khola section mudstone samples, a single Surai Khola conglomerate matrix sample and quartzite clasts from all three sections, compared with typical values for major Himalayan tectonic zones. Two Surai Khola clasts with εNd/Sr values of −21.9/0.934 and −18/0.875 fall outside the limits of the plot due to their high Sr values. Modified from White *et al.* (2002). Ellipses illustrate 1 σ distributions of fields, Lesser Himalayan $^{87}Sr/^{86}Sr$ ratios > 2 are excluded from the plot and εNd values restricted to the Inner Lesser Himalaya. Published values are recalculated to $t = 0$ where necessary. Data from Derry & France-Lanord (1996), Najman *et al.* (2000); Parrish & Hodges (1996), Richards *et al.* (2005); Ahmad *et al.* (2000), Robinson *et al.* (2001).

represents a maximum value, with the prospect that younger grains are present in the sample but not analysed. Typical uncertainties are in the range of 0.2–1 Ma (2σ) for SUERC ages and 0.5–5 Ma for MIT ages (2σ), the differences arising from the working accuracy of the respective mass spectrometers. Cumulative probability plots of the postcollision ages (< 50 Ma; > 95% of detrital grains) reveal Gaussian age distributions with a total combined mode of 16.8 Ma (Fig. 9). The highest age frequency generally falls between 20 and 15 Ma. The youngest micas tend to be in lowest abundance (53 grains aged 14–15 Ma, 34 grains aged 13–14 Ma, nine grains aged 12–13 Ma, three grains aged 11–12 Ma and three grains, two with high errors, aged

Table 2. Step heating results for Surai Khola detrital white micas

Sample	Stratigraphic age (Ma)	Plateau age (Ma) error	MSWD
SKA14	1	15.89 ± 0.12	1.92
SKA14	1	15.84 ± 0.24	0.84
SKA14	1	14.80 ± 0.16	1.10
SKA14	1	16.14 ± 0.20	1.52
SKA14	1	15.48 ± 0.01	0.79
SK2760	5	16.81 ± 0.18	2.16
SK2760	5	15.15 ± 0.20	2.03
SK2760	5	14.97 ± 0.17	1.25
SK2760	5	20.08 ± 0.13	1.11
SK2760	5	15.07 ± 0.11	1.25
SK1780	7	17.15 ± 0.29	1.80
SK1780	7	17.90 ± 0.43	0.63
SK1780	7	16.50 ± 0.32	0.33
SK1780	7	17.13 ± 0.18	0.55
SK1448	7.8	18.29 ± 0.15	0.44
SK1448	7.8	16.04 ± 0.17	0.22

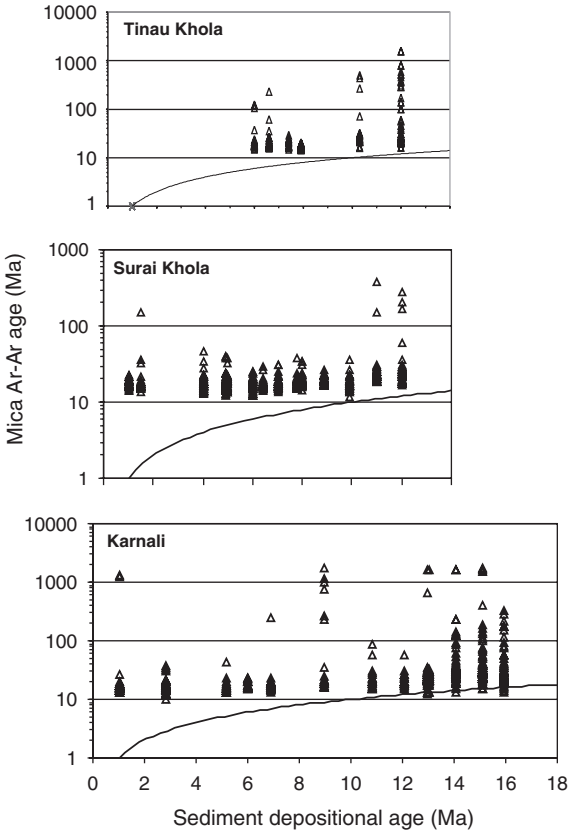

Fig. 8. Detrital white mica cooling ages vs. the stratigraphic age of the host sediment. Curved line represents zero-age lag times where mica age equals sedimentary age and so mica ages should lie above this line. Two white micas for the 16 Ma Karnali sample plot below the 1 : 1 line and are not within error of a zero-age lag time. This could be due to some kind of alteration but they are only two in a data set of 1415 white micas. The modal age for Tinau Khola is 17.8 Ma and for Surai Khola and Karnali is 16.8 Ma.

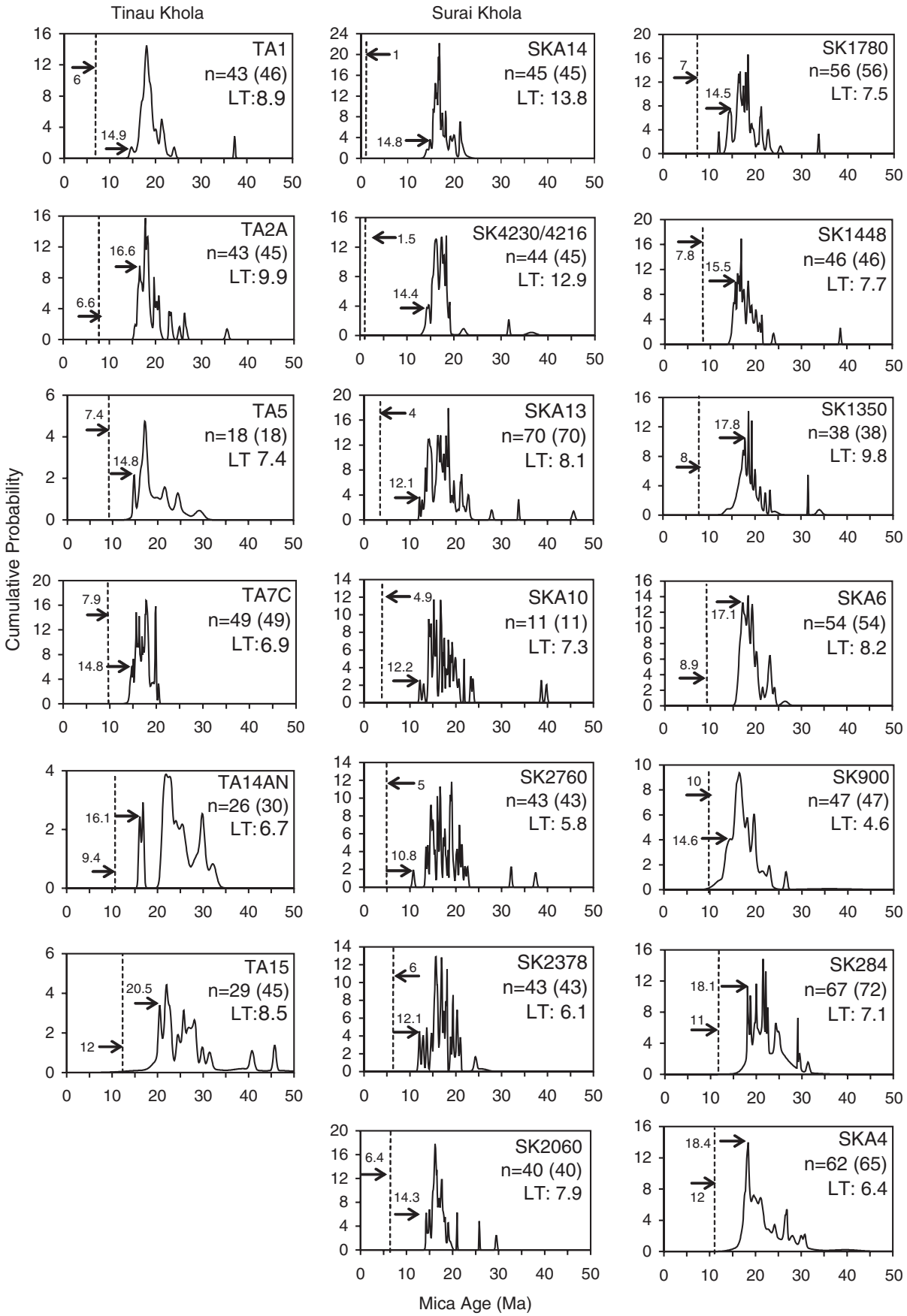

Fig. 9. Cumulative probability plots of detrital white mica ages. The dashed line shows the host sediment depositional age, also indicated by arrow (in Ma). Arrow also indicates the age (in Ma) of the chosen youngest peak for determining lag time. Sample age increases from top to bottom. For sample numbers TA, Tinau Khola; SK, Surai Khola; K, Karnali; *n*, number of dated grains younger than 50 Ma; (*n*), total number of dated grains; LT, lag time for youngest peak age.

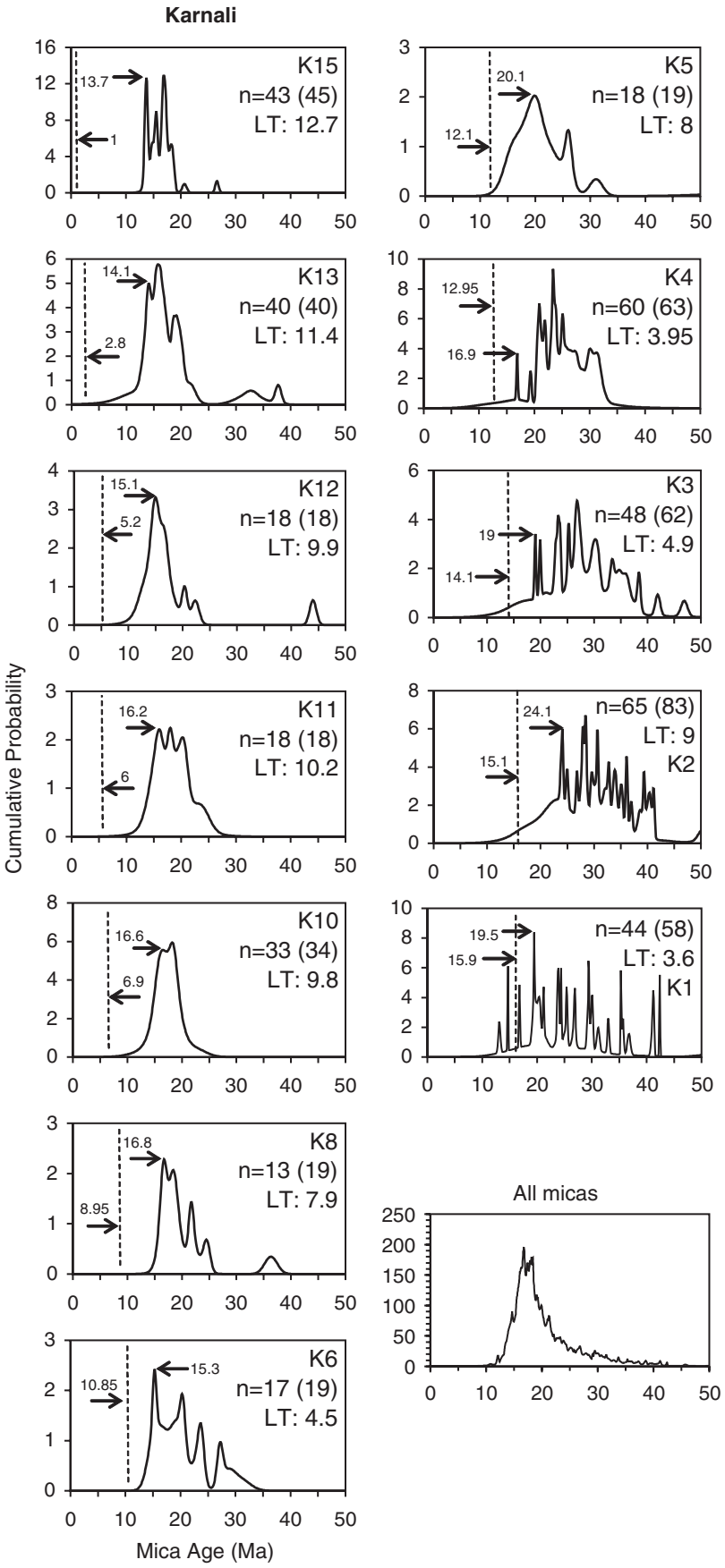

Fig. 9. (*Continued*)

10–11 Ma). Pre-Himalayan ages span back to 1200 Ma, reflecting thermal histories before the India-Asia collision, and are more abundant in sediment deposited at 12 Ma and older. The plots do not show major differences between samples except a significantly older age population for the oldest Karnali samples and as such suggest that the crust of the respective source areas was similar and underwent the same exhumation history. In spite of high scatter of data, a trend of decreasing youngest peak age with time can be seen in the Karnali section. This trend is not so clearly defined in the Surai Khola or Tinau Khola sections. Lag times generally increase with time (Karnali and Surai Khola sections), and no lag times shorter than 5.8 m.y. are found after ~10 Ma. Shortest lag times are found in the Karnali section; 3.6 m.y. lag time for sediment deposited at 16 Ma, 4 m.y. for sediment deposited at 13 Ma and 4.5 m.y. for that deposited at 11 Ma (Fig. 9). The Surai Khola micas reveal short lag times at 12 Ma (6.4 m.y.) and again at 10 Ma (4.6 m.y.). The Tinau Khola section has a minimum lag time at 10 Ma (6.7 m.y.). Lag times increase significantly to 13.8. and 12.7 m.y. for the Surai Khola and Karnali sections, respectively, by 1 Ma.

DISCUSSION

Provenance

Petrographic modes of sandstones suggest that sedimentary to low-grade metamorphic detritus dominated the supply of sediment to the foreland basin (~90%) throughout deposition of the Karnali, Surai Khola and Tinau Khola sections. In contrast, ε_{Nd} values of −17 for mudstone samples indicate dominant derivation from either the Tethyan /Tibetan Himalayan Zone or the Greater Himalaya, which now forms the high-grade metamorphic core of the mountain range. Considering the geographical region exhuming rapidly at the time lay south of the STDZ, the most likely source, that could produce these two detrital signatures, is the low-grade Greater Himalayan protolith/cover, such as the variously named Haimanta, Kade Formation or Chamba sequence in NW India (Pognante *et al*., 1990; Thakur, 1998; Walker *et al*., 1999) or the Sanctuary Formation of Nepal (Colchen *et al*., 1986; Table 1). These rocks are likely to have been more extensive in the past and probably remained a major source area throughout Siwalik deposition as deduced from the homogeneity of the petrography and geochemistry data. Similar reasons led White *et al*. (2002) to invoke a Haimanta source area for the post-17 Ma foreland basin sediments of the Dharamsala Group, NW India. It is less likely that the data can be explained by invoking different provenances for the two grain size fractions because geochemical analysis of Surai Khola and Karnali sandstones by Huyghe *et al*. (2001, 2005) yielded similar results to this mudstone study. The metamorphosed Greater Himalaya must have been the main source for the postcollision aged (< 50 Ma) white micas. Older precollision aged micas could have been derived from a Lesser Himalayan, Tibetan Himalayan or Greater Himalayan protolith or cover source area but the small number of old grains and the absence of a distinct age group restricts their use as a provenance indicator. Our data therefore suggest that during Siwalik deposition, sediment was mostly derived from Greater Himalayan low grade protolith/cover and high-grade metamorphic rocks, with input from the Lesser Himalaya increasing through time.

The proportion of sedimentary detritus increases at 12 Ma in the Karnali section as does the amount of carbonate material, typical of the Lesser Himalaya. There is also a subtle increase in $^{87}Sr/^{86}Sr$ from 12 Ma onwards, while Huyghe *et al*. (2001) and Robinson *et al*. (2001) report increasingly negative ε_{Nd} values for the Surai Khola and Karnali sections after 12 Ma. Assuming average ε_{Nd} values of −15 for the Greater Himalaya and Greater Himalayan protolith/cover and −25 for the Lesser Himalaya, a value of −17 indicates a contribution of ~18–20% from the Lesser Himalayan Zone using equation (3) from Vance *et al*. (2003) and their calculated erosion rates. The relatively low abundance of mica and monazite in the Lesser Himalaya (minerals that have a strong control on detrital Nd geochemistry), and high abundance of carbonate that could be lost in solution, means that the Greater Himalaya would have a tendency to swamp the mixed geochemical signal. Our evidence for more negative (−18 to −30) Lesser Himalayan ε_{Nd} values in clasts, back to 6.7 Ma in the Tinau Khola section, 6 Ma in the Karnali section and 4.8 Ma in the Surai Khola section (no clasts occur in the older part of the sediment section), provides further evidence for erosion of the Lesser Himalaya by those times. The combination of these up-section changes points to a gradually increasing contribution from the Lesser Himalaya after 12 Ma, a scenario that conforms with current tectonic evolutionary models in which the Lesser Himalayan duplex is exposed from ~12 Ma (e.g. DeCelles *et al*., 2001). The lack of a concurrent switch to a greater proportion of Lesser Himalayan-type old mica grains is probably due to the relatively low mica abundance in the Lesser Himalayan rocks and the smaller grain size of older micas inducing a sampling bias. A combination of increasing feldspar and garnet between 9 and 6 Ma hints at an increasing contribution from the Greater Himalaya, perhaps reflecting a deepening of the erosion level into high-grade Greater Himalayan rocks as recorded by heavy mineral trends (Fig. 6m). The evolution of heavy mineral suites from staurolite to dominantly kyanite between 8 and 7 Ma and increase in MI in all three sections suggests more extensive erosion of amphibolite-facies metasediments in the drainage basin during this period. However, it is important to note that an up-section decrease in diagenetic dissolution can mimic the gradual unroofing trend seen from ~10 Ma to the present (Morton, 1985). The superposition of these two effects hampers a straightforward reconstruction of tectonic or erosional histories from heavy mineral suites. In Nepal, the Dumri Formation molasse (age ~20–15 Ma) lacks both high-grade minerals and medium- to high-grade lithic material (DeCelles *et al*.,

1998a) and thus our data from the Siwalik succession record the time when the highest-grade rocks first became exposed. DeCelles *et al.* (1998b) found kyanite and sillimanite from the Khutia Khola section in far western Nepal at ~11 Ma, indicating some variation along the strike.

Exhumation

In Northern India, White *et al.* (2002) documented essentially zero-aged lag times from micas in the foreland basin sediments aged 20–17 Ma, indicating extremely rapid exhumation. Using simple one-dimensional (1D) thermal modelling, they calculated exhumation rates of up to 5 mm year^{-1} for the Greater Himalaya at 20 Ma, subsequently slowing to 1 mm year^{-1}. We use the 1D thermal modelling described in White (2002) and Vance *et al.* (2003), which takes into account advective perturbation of the geothermal gradient within the thickened crust. The model assumes a white mica closure temperature of 400 °C and that an equilibrium geotherm was reached a few million years after exhumation began, where $T = 700$ °C at 35 km depth. Our shortest lag time of 3.6 Myr at 16 Ma equates to an exhumation rate of 2.6 mm year^{-1} for the Greater Himalaya. After ~10 Ma there are no lag times shorter than 5.8 Ma (lag time of 4.6 Myr at 10 Ma corresponds to an exhumation rate of 3.3 mm year^{-1}) and subsequent exhumation was slower with a mean of 1.5 mm year^{-1}. A limitation of the 1D model is that it does not take into account transient changes in exhumation rate or conductive heat loss or gain. It has also been shown that micas grow above and below the stated closure temperature (Villa, 1997; Di Vincenzo *et al.*, 2001) and the ^{40}Ar–^{39}Ar ages obtained could represent not only cooling due to exhumation, but also fluid flow, deformation or retrograde mineral reactions (Hames & Cheney, 1997; Muller *et al.*, 1999; Glodny *et al.*, 2002). Nevertheless, we interpret the mica ages recorded here as the timing of cooling through the ^{40}Ar–^{39}Ar closure temperature due to exhumation as the ages concord well with those in the hinterland which are geographically widespread, widely interpreted as the result of exhumation and contain few anomalous ages. The highest detrital white mica age frequency falls between 20 and 15 Ma with a mode of 16.8 Ma (Fig. 9). This indicates the period of most rapid Greater Himalayan unroofing, whereby maximum erosion is associated with maximum exhumation, and correlates well with isotope data from the hinterland. Decreasing youngest peak ages indicate continued exhumation into deeper levels of the Greater Himalaya throughout the period under study, while increasing lag times indicate that exhumation of the Greater Himalaya was slowing down. The fact that there are no micas younger than 10–12 Ma, no lag times less than 6 Myr after 10 Ma and there is a change of provenance at ~12 Ma indicates that this period represents the time of transference of exhumation south of the Greater Himalaya. Although mica ages < 10 Ma are found in the Greater Himalaya (Brewer *et al.*, 2003, and Fig. 1 with references therein), these grains appear to be concentrated for the large part in the lowest regions of the Greater Himalayan Thrust Sheet and Main Central Thrust Zone. This spatial restriction, coupled with the fact that many of the grains are younger than the depositional age of the youngest Siwalik sedimentary rock we sampled, explains the lack of these young grains in our Siwalik study.

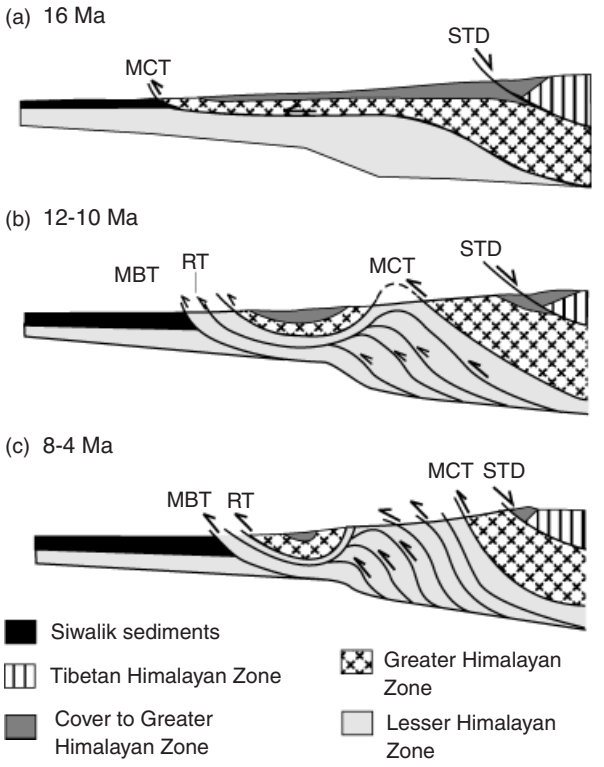

Fig. 10. Schematic cross-sections through the central Himalayas to show orogenic evolution during Siwalik deposition. Adapted from DeCelles *et al.* (1998b). STD, South Tibetan Detachment; MCT, Main Central Thrust; RT, Ramgarh Thrust; MBT, Main Boundary Thrust; THZ, Tibetan Himalayan Zone; GHZ, Greater Himalayan Zone; LHZ, Lesser Himalayan Zone.

CONCLUSIONS

During the period under study, maximum exhumation rates of the Greater Himalaya occurred at ~16 Ma, as evidenced by the greatest frequency of mica ages and the shortest lag times. From 12 Ma and by 10 Ma the orogen (at least in the central Himalaya) underwent a dramatic reorganisation whereby the locus of strain accommodation switched from the Main Central Thrust to structures within the Lesser Himalayan duplex. This is evidenced by provenance data, which indicates Lesser Himalayan input at this time, a lack of any micas younger than 12–10 Ma and a lack of lag times of less than 6 m.y. after 10 Ma. We therefore record progressive southward growth of the orogenic wedge from 12 Ma onwards through the accretion of new structures towards the foreland, as summarised in Fig. 10. Greater Himalayan low-grade protolith/cover material contributed to the majority of foreland-bound sediment throughout the Siwalik deposition. Our conclusions are

supported by consistent data from all three Siwalik sections, suggesting a lateral continuity in tectonic evolution for the central Himalayas and the absence of processes that hinder the use of the detrital technique to document hinterland tectonics, such as sediment ponding and drainage diversion. This work emphasises the utility of combining both a range of procedures and more than one time-equivalent sedimentary section when employing the detrital approach.

REFERENCES

Ahmad, T., Harris, N., Bickle, M., Chapman, H., Bunbury, J. & Prince, C. (2000) Isotopic constraints on the structural relationships between the Lesser Himalayan Series and the High Himalayan Crystalline Series, Garhwal Himalaya. *Geol. Soc. Am. Bull.*, **112**, 467–477.

Aitchison, J.C. (1986) Stratigraphy, sedimentology and tectonic evolution of the Shimanto Terrane, Southwest Japan. *Chikyu Kagaku – (Earth Sci.)*, **40**, 337–363.

Allen, P.A., Homewood, P. & Williams, G.D. (1986) Foreland basins: an introduction. In: *Foreland Basins* (Ed. By P.A. Allen & P. Homewood), pp. 3–12. Blackwell Scientific Publications, Oxford.

Amatya, K. & Jnawali, B. (1994) Geological map of Nepal, DMG/ICIMOD/DCG/UNEP, scale 1:1 000 000.

Appel, E., Roesler, W. & Corvinus, G. (1991) Magnetostratigraphy of the Miocene–Pleistocene Surai Khola Siwaliks in West Nepal. *Geophys. J. Int.*, **105**, 191–198.

Beaumont, C., Jamieson, R.A., Nguyen, M.H. & Lee, B. (2001) Himalayan tectonics explained by extrusion of a low-viscosity crustal channel coupled to focused surface denudation. *Nature*, **414**, 738–742.

Bernet, M. & Spiegel, C. (2004) Introduction: Detrital thermochronology. In: *Detrital Thermochronology – Provenance analysis, Exhumation and Landscape Evolution of Mountain Belts* (Ed. By M. Bernet & C. Speigel) Geological Society of America Special Publication, **378**, 1–8.

Bickle, M.J., Wickham, S.M., Chapman, H.J. & Taylor, H.P. Jr. (1988) A strontium, neodymium and oxygen isotope study of hydrothermal metamorphism and crustal anatexis in the Trois Seigneurs Massif, Pyrenees, France. *Cont. Min. Petrol.*, **100**, 399–417.

Bollinger, L., Avouac, J.P., Beyssac, O., Catlos, E.J., Harrison, T.M., Grove, M., Goffe, B. & Sapkota, S. (2004) Thermal structure and exhumation history of the Lesser Himalaya in central Nepal. *Tectonics*, **23**, TC5015, doi:10.1029/2003TC001564.

Bollinger, L. & Janots, E. (2006) Evidence for Mio-Pliocene retrograde monazite in the Lesser Himalaya, far western Nepal. *Eur. J. Mineral.*, **18**, 289–297.

Brewer, I.D., Burbank, D.W. & Hodges, K.V. (2003) Modelling detrital cooling-age populations; insight from two Himalayan catchments. *Basin Research*, **15**, 305–320.

Burbank, D.W., Beck, R.A. & Mulder, T. (1996) The Himalayan foreland basin. In: *The Tectonic Evolution of Asia* (Ed. By A. Yin & T.M. Harrison), pp. 149–188. Cambridge University Press, New York.

Burchfiel, B.C., Chen, Z., Hodges, K.V., Liu, Y., Royden, L.H., Deng, C. & Xu, J. (1992) The South Tibetan detachment system, Himalayan Orogen; extension contemporaneous with and parallel to shortening in a collisional mountain belt. *Geol. Soc. Am. Spec. Pap.*, **269**, p. 41..

Burg, J.P. & Chen, G.M. (1984) Tectonics and structural zonation of southern Tibet, China. *Nature*, **311**, 219–223.

Butler, R.F. (1992) *Paleomagnetism: Magnetic Domains to Geologic Terranes*. Blackwell Scientific Publications, Boston, 319pp.

Cande, S.C. & Kent, D.V. (1995) Revised calibration of the geomagnetic polarity timescale for the Late Cretaceous and Cenozoic. *J. Geophys. Res.*, **100**, 6093–6095.

Catlos, E.J., Harrison, T.M., Kohn, M.J., Grove, M., Ryerson, F.J., Manning, C.E. & Upreti, B.N. (2001) Geochronologic and thermobarometric constraints on the evolution of the Main Central Thrust, central Nepal Himalaya. *J. Geophys. Res.*, **106**, 16177–16204.

Catlos, E.J., Harrison, T.M., Manning, C.E., Grove, M., Rai, S.M., Hubbard, M.S. & Upreti, B.N. (2002) Records of the evolution of the Himalayan orogen from in situ Th–Pb ion microprobe dating of monazite: Eastern Nepal and western Garhwal. *J. Asian Earth Sci.*, **20**, 459–479.

Chauvel, C. & Blichert-Toft, J. (2001) A hafnium and trace element perspective on melting of the depleted mantle. *Earth Planet. Sci. Lett.*, **190**, 137–151.

Colchen, M., Le Fort, P. & Pecher, A. (1986) Geological research in the Nepal Himalayas, Annapurna, Manaslu, Ganesh Himal; 1:20,000 geological map. *Cent. Natl. Rech. Sci., Paris*, p. 137.

Coleman, M.E. (1996) Orogen-parallel and orogen-perpendicular extension in the central Nepalese Himalayas. *Geol. Soc. Am. Bull.*, **108**, 1594–1607.

Coleman, M.E. & Hodges, K.V. (1998) Contrasting Oligocene and Miocene thermal histories from the hanging wall and footwall of the South Tibetan detachment in the central Himalaya from $^{40}Ar/^{39}Ar$ thermochronology, Marsyandi Valley, central Nepal. *Tectonics*, **17**, 726–740.

Copeland, P. & Harrison, T.M. (1990) Episodic rapid uplift in the Himalaya revealed by $^{40}Ar/^{39}Ar$ analysis of detrital K-feldspar and muscovite, Bengal Fan. *Geology*, **18**, 354–357.

Copeland, P., Harrison, T.M., Hodges, K.V., Maruejol, P., Le Fort, P. & Pecher, A. (1991) An early Pliocene thermal disturbance of the Main Central Thrust, central Nepal; implications for Himalayan tectonics. *J. Geophys. Res.*, **96**, 8475–8500.

Copeland, P., LeFort, P., Ray, S.M. & Upreti, B.N. (1996) Cooling history of the Kathmandu crystalline nappe: $^{40}Ar/^{39}Ar$ results. Enriched: 30th International Geological Congress; Abstracts, 30, p. 197.

Coward, M.P. & Butler, R.H.W. (1985) Thrust tectonics and the deep structure of the Pakistan Himalaya. *Geology*, **13**, 417–420.

Daniel, C.G., Hollister, L.S., Parrish, R.R. & Grujic, D. (2003) Exhumation of the Main Central Thrust from Lower Crustal Depths, Eastern Bhutan Himalaya. *J. Met. Geol.*, **21**, 317–334.

DeCelles, P.G., Garzione, C.N., Copeland, P., Upreti, B.N., Robinson, D.M., Quade, J. & Ojha, T.P. (2001) Stratigraphy, structure, and tectonic evolution of the Himalayan fold-thrust belt in Western Nepal. *Tectonics*, **20**, 487–509.

DeCelles, P.G., Gehrels, G.E., Najman, Y., Martin, A.J., Carter, A. & Garzanti, E. (2004) Detrital geochronology and geochemistry of Cretaceous–Early Miocene strata of Nepal: implications for timing and diachroneity of initial Himalayan orogenesis. *Earth Planet. Sci. Lett.*, **227**, 313–330.

DeCelles, P.G., Gehrels, G.E., Quade, J. & Ojha, T.P. (1998a) Eocene–early Miocene foreland basin development and the

history of Himalayan thrusting, western and central Nepal. *Tectonics*, **17**, 741–765.

DeCelles, P.G., Gehrels, G.E., Quade, J., Ojha, T.P., Kapp, P.A. & Upreti, B.N. (1998b) Neogene foreland basin deposits, erosional unroofing, and the kinematic history of the Himalayan fold-thrust belt, western Nepal. *Geol. Soc. Am. Bull.*, **110**, 2–21.

Derry, L.A. & France-Lanord, C. (1996) Neogene Himalayan weathering history and river $^{87}Sr/^{86}Sr$; impact on the marine Sr record. *Earth Planet. Sci. Lett.*, **142**, 59–74.

Dettman, D.L., Kohn, M.J., Quade, J., Ryerson, F.J., Ojha, T.P. & Hamidullah, S. (2001) Seasonal stable isotope evidence for a strong Asian monsoon throughout the past 10.7 m.y. *Geology*, **29**, 31–34.

Dewey, J.F., Cande, S.C. & Pitman, W.C. (1989) Tectonic evolution of the India/Eurasia collision zone. *Eclo. Geol. Helv.*, **82**, 717–734.

Dickinson, W.R. (1985) Interpreting provenance relations from detrital modes of sandstones. In: *Provenance of Arenites* (Ed. by G.G. Zuffa), pp 333–361. D. Reidel Publishing Company, Dordrecht.

Dickinson, W.R., Beard, L.S., Brakenridge, G.R., Erjavec, J.L., Ferguson, R.C., Inman, K.F., Knepp, R., Lindberg, F.A. & Ryberg, P.T. (1983) Provenance of North American Phanerozoic sandstones in relation to tectonic setting. *Geol. Soc. Am. Bull.*, **94**, 222–235.

Di Vincenzo, G., Ghiribelli, B., Giorgetti, G. & Palmeri, R. (2001) Evidence of a close link between petrology and isotope records: constraints from SEM, EMP, TEM and in situ ^{40}Ar–^{39}Ar laser analyses on multiple generations of white micas (Lanterman Range, Antarctica). *Earth Planet. Sci. Lett.*, **192**, 389–405.

Edwards, R.M. (1995) $^{40}Ar/^{39}Ar$ geochronology of the Main Central Thrust (MCT) region; evidence for late Miocene to Pliocene disturbances along the MCT, Marsyangdi River valley, west-central Nepal Himalaya. *J. Nepal Geol. Soc.*, **10**, 41–46.

France-Lanord, C., Derry, L. & Michard, A. (1993) Evolution of the Himalaya since Miocene time: isotopic and sedimentological evidence from the Bengal Fan. In: *Himalayan Tectonics* (Ed. by P.J. Treloar & M.P. Searle), *Geol. Soc. Lond.*, **74**, 603–621.

Gaetani, M. & Garzanti, E. (1991) Multicyclic history of the northern India continental margin (northwestern Himalaya). *AAPG Bull.*, **75**, 1427–1446.

Galy, A., France-Lanord, C. & Derry, L.A. (1996) The late Oligocene-early Miocene Himalayan belt; constraints deduced from isotopic compositions of early Miocene turbidites in the Bengal Fan. *Tectonophysics*, **260**, 109–118.

Galy, A. (1999) Etude géochimique de l'érosion actuelle de la chaîne himalayenne. PhD Thesis, Institut National Polytechnique de Lorraine, Nancy, p. 466.

Garver, J.I., Brandon, M.T., Roden-Tice, M.K. & Kamp, P.J.J. (1999) Exhumation history of orogenic highlands determined by detrital fission-track thermochronology. In: *Exhumation Processes; Normal Faulting, Ductile Flow and Erosion* (Ed. by U. Ring, M.T. Brandon, G.S. Lister & S.D. Willett), *Geol. Soc. Lond. Spec. Pub.*, **154**, 283–304.

Garzanti, E. (1999) Stratigraphy and sedimentary history of the Nepal Tethys Himalaya passive margin. *J. Asian Earth Sci.*, **17**, 805–827.

Garzanti, E., Baud, A. & Mascle, G. (1987) Sedimentary record of the northward flight of India and its collision with Eurasia (Ladakh Himalaya, India). *Geodinamica Acta*, **1**, 297–312.

Garzanti, E., Critelli, S. & Ingersoll, R.V. (1996) Paleogeographic and paleotectonic evolution of the Himalayan Range as reflected by detrital modes of Tertiary sandstones and modern sands (Indus transect, India and Pakistan). *Geol. Soc. Am. Bull.*, **108**, 631–642.

Garzanti, E. & Van Haver, T. (1988) The Indus clastics; forearc basin sedimentation in the Ladakh Himalaya (India). *Sediment. Geol.*, **59**, 237–249.

Garzanti, E. & Vezzoli, G. (2003) A classification of metamorphic grains in sands based on their composition and grade. *J. Sediment. Res.*, **73**, 830–837.

Gautam, P. & Appel, E. (1994) Magnetic-polarity stratigraphy of Siwalik Group sediments of Tinau Khola section in west central Nepal, revisited. *Geophys. J. Int.*, **117**, 223–234.

Gautam, P. & Fujiwara, Y. (2000) Magnetic polarity stratigraphy of Siwalik Group sediments of Karnali River section in western Nepal. *Geophys. J. Int.*, **142**, 812–824.

Gautam, P. & Rosler, W. (1999) Depositional chronology and fabric of Siwalik group sediments in Central Nepal from magnetostratigraphy and magnetic anisotropy. *J. Asian Earth Sci.*, **17**, 659–682.

Glodny, J., Bingen, B., Austrheim, H., Molina, J.F. & Rusin, A. (2002) Precise eclogitization ages deduced from Rb/Sr mineral systematics: the Maksyutov complex, Southern Urals, Russia. *Geochim. Cosmochim. Acta*, **66**, 1221–1235.

Godin, L., Brown, R.L. & Hanmer, S. (1999) High strain zone in the hanging wall of the Annapurna Detachment, central Nepal Himalaya. In: *Himalaya and Tibet; mountain roots to mountain tops* (Ed. by A. Macfarlane, R.B. Sorkhabi & J. Quade), *Geol. Soc. Am., Boulder.*, **328**, 199–210.

Godin, L., Parrish, R.R., Brown, R.L. & Hodges, K.V. (2001) Crustal thickening leading to exhumation of the Himalayan metamorphic core of central Nepal; insight from U–Pb geochronology and $^{40}Ar/^{39}Ar$ thermochronology. *Tectonics*, **20**, 729–747.

Goldstein, S.L., O'Nions, R.K. & Hamilton, P.J. (1984) A Sm–Nd isotopic study of atmospheric dusts and particulates from major river systems. *Earth Planet. Sci. Lett.*, **70**, 221–236.

Hames, W.E. & Cheney, J.T. (1997) On the loss of ^{40}Ar from muscovite during polymetamorphism. *Geochim. Cosmochim. Acta*, **61**, 3863–3872.

Harrison, T.M., Copeland, P., Hall, S.A., Quade, J., Burner, S., Ojha, T.P. & Kidd, W.S.F. (1993) Isotopic preservation of Himalayan/Tibetan uplift, denudation, and climatic histories of two molasses deposits. *J. Geol.*, **101**, 157–175.

Harrison, T.M., Copeland, P., Kidd, W.S.F. & Yin, A. (1992) Raising Tibet. *Science*, **255**, 1663–1670.

Harrison, T.M., Ryerson, F.J., Le Fort, P., Yin, A., Lovera, O.M. & Catlos, E.J. (1997) A late Miocene–Pliocene origin for the central Himalayan inverted metamorphism. *Earth Planet. Sci. Lett.*, **146**, E1–E7.

Hauck, M.L., Nelson, K.D., Brown, L.D., Zhao, W. & Ross, A.R. (1998) Crustal structure of the Himalayan orogen at approximately 90° east longitude from Project INDEPTH deep reflection profiles. *Tectonics*, **17**, 481–500.

Hodges, K.V. (2000) Tectonics of the Himalaya and southern Tibet from two perspectives. *Geol. Soc. Am. Bull.*, **112**, 324–350.

Hodges, K.V., Parrish, R.R., Housh, T.B., Lux, D.R., Burchfiel, B.C., Royden, L.H. & Chen, Z. (1992) Simultaneous Miocene extension and shortening in the Himalayan Orogen. *Science*, **258**, 1466–1470.

Hodges, K.V., Parrish, R.R. & Searle, M.P. (1996) Tectonic evolution of the central Annapurna Range, Nepalese Himalaya. *Tectonics*, **15**, 1264–1291.

Honegger, K., Dietrich, V., Frank, W., Gansser, A., Thoeni, M. & Trommsdorff, V. (1982) Magmatism and metamorphism in the Ladakh Himalayas (the Indus–Tsangpo suture zone). *Earth Planet. Sci. Lett.*, **60**, 253–292.

Hubbard, M.S. & Harrison, T.M. (1989) $^{40}Ar/^{39}Ar$ age constraints on deformation and metamorphism in the Main Central Thrust zone and Tibetan Slab, eastern Nepal Himalaya. *Tectonics*, **8**, 865–880.

Huyghe, P., Galy, A., Mugnier, J.-L. & France-Lanord, C. (2001) Propagation of the thrust system and erosion in the Lesser Himalaya: Geochemical and sedimentological evidence. *Geology*, **29**, 1007–1010.

Huyghe, P., Mugnier, J.L., Gajurel, A.P. & Delcaillau, B. 2005 Tectonic and climatic control of the changes in the sedimentary record of the Karnali River section (Siwaliks of Western Nepal). *The Island Arc*, **14**, 311–327.

Ingersoll, R.V., Pickle, J.D., Sares, S.W., Bullard, T.F., Ford, R.L. & Grimm, J.P. (1984) The effect of grain size on detrital modes: a test of the Gazzi–Dickinson pointcounting method (Holocene, sand, New Mexico, USA). *J. Sediment. Petrol.*, **54**, 103–116.

Johnson, M.R.W. (2003) Insight into the nature of Indian crust underthrusting the Himalaya. *Terra Nova*, **15**, 46–51.

Klootwijk, C.T., Gee, J.S., Peirce, J.W., Smith, G.M. & McFadden, P.L. (1992) An early India-Asia contact; paleomagnetic constraints from Ninetyeast Ridge, ODP Leg 121; with Suppl. Data 92–15. *Geology*, **20**, 395–398.

Kohn, M.J., Catlos, E.J., Ryerson, F.J. & Harrison, T.M. (2001) Pressure-temperaturetime path discontinuity in the Main Central Thrust zone, central Nepal. *Geology*, **29**, 571–574.

Lavé, J. & Avouac, J.P. (2000) Active folding of fluvial terraces across the Siwaliks Hills, Himalayas of central Nepal. *J. Geophys. Res.*, **105**, 5735–5770.

Macfarlane, A.M. (1993) Chronology of tectonic events in the crystalline core of the Himalaya, Langtang National Park, central Nepal. *Tectonics*, **12**, 1004–1025.

Maluski, H., Matte, P., Brunel, M. & Xiao, X. (1988) $^{40}Ar/^{39}Ar$ dating of metamorphic and plutonic events in the North and High Himalaya belts (southern Tibet, China). *Tectonics*, **7**, 299–326.

Manage, M.A. & Maurer, H.F.W. (1992) *Heavy minerals in colour*. Chapman & Hall, London, p. 147.

Meigs, A.J., Burbank, D.W. & Beck, R.A. (1995) Middle-late Miocene (> 10 Ma) formation of the Main Boundary Thrust in the western Himalaya. *Geology*, **23**, 423–426.

Metcalf, R.P. (1993) Pressure, temperature and time constraints on metamorphism across the Main Central thrust zone and high Himalayan slab in the Garhwal Himalaya. In: *Himalayan Tectonics* (Ed. by P.J. Treloar & M.P. Searle), *Geol. Soc. Lond. Spec. Pub.*, **74**, 485–509.

Morton, A. (1985) Heavy minerals in provenance studies. In: *Provenance of Arenites. NATO ASI Series C: Mathematical and Physical Sciences*, **Vol. 148** (Ed. By G.G. Zuffa), pp 249–277. D. Reidel Publishing Company, Dordrecht.

Mugnier, J.-L., Huyghe, P., Chalaron, E., Vidal, G., Husson, L., Delcaillau, B., Leturmy, P. & Mascle, G. (1999) The Siwaliks of western Nepal I. Geometry and kinematics. *J. Asian Earth Sci.*, **17**, 629–642.

Mugnier, J.-L., Huyghe, P., Leturmy, P. & Jouanne, F. (2004) Episodicity and rates of thrust sheet motion in Himalaya (Western Nepal). In: *Thrust Tectonics and Hydrocarbon Systems* (Ed. by K.R. McClay), *AAPG Memoir,* **82**, 91–114.

Mugnier, J.-L., Mascle, G. & Faucher, T. (1993) Structure of the Siwaliks of western Nepal: an intracontinental accretionary prism. *Int. Geol. Rev.*, **35**, 1–16.

Muller, W., Dallmeyer, D., Neubauer, F. & Thoni, M. (1999) Deformation-induced resetting of Rb/Sr and $^{40}Ar/^{39}Ar$ mineral systems in a low-grade, polymetamorphic terrane (Eastern Alps, Austria). *J. Geol. Soc. Lond.*, **156**, 261–278.

Murphy, M.A. & Yin, A. (2003) Structural evolution and sequence of thrusting in the Tethyan fold-thrust belt and Indus-Yalu suture zone, southwest Tibet. *Geol. Soc. Am. Bull.*, **115**, 21–34.

Najman, Y., Bickle, M. & Chapman, H. (2000) Early Himalayan exhumation: constraints from the Indian foreland basin. *Terra Nova*, **12**, 28–34.

Najman, Y. & Garzanti, E. (2000) Reconstructing early Himalayan tectonic evolution and paleogeography from Tertiary foreland basin sedimentary rocks, northern India. In: *Special focus on the Himalaya* (Ed. by J.W. Geissman & A.F. Glazner), *Geol. Soc. Am. Boulder,* **112**, 435–449.

Najman, Y., Johnson, C., White, N.M. & Oliver, G. (2004) Evolution of the Himalayan foreland basin, NW India. *Basin Res.*, **16**, 1–24.

Najman, Y., Pringle, M.S., Johnson, M.R.W., Robertson, A.H.F. & Wijbrans, J.R. (1997) Laser $^{40}Ar/^{39}Ar$ dating of single detrital muscovite grains from early foreland basin sedimentary deposits in India; implications for early Himalayan evolution. *Geology*, **25**, 535–538.

Nakayama, K. & Ulak, P.D. (1999) Evolution of fluvial style in the Siwalik Group in the foothills of the Nepal Himalaya. *Sediment. Geol.*, **125**, 205–224.

Ojha, T.P., Butler, R.F., Quade, J., DeCelles, P.G., Richards, D. & Upreti, B.N. (2000) Magnetic polarity stratigraphy of the Neogene Siwalik Group at Khutia Khola, far western Nepal. In: *Special Focus on the Himalaya* (Ed. by J.W. Geissman & A.F. Glazner), *Geol. Soc. Am., Boulder* **112**, 424–434.

Ojha, T.P., Butler, R.F., Quade, J., DeCelles, P.G. & Upreti, B.N. (2001) Magnetic polarity stratigraphy of foreland basin sediments of Nepal Himalaya. *J. Asian Earth Sci.*, **19**, special abstracts issue (HKT16), 48–49.

Parfenoff, A., Pomerol, C. & Tourenq, J. (1970) Mineral grains; methods of study and determination. Masson et Cie, Paris, p. 574.

Parkash, B., Sharma, R.P. & Roy, A.K. (1980) The Siwalik Group (molasse), – sediments shed by collision of continental plates. *Sediment. Geol.*, **25**, 127–159.

Parrish, R.R. & Hodges, K.V. (1996) Isotopic constraints on the age and provenance of the Lesser and Greater Himalayan sequences, Nepalese Himalaya. *Geol. Soc. Am. Bull.*, **108**, 904–911.

Paudel, L.P. & Arita, K. (2000) Tectonic and polymetamorphic history of the Lesser Himalaya in central Nepal. *J. Asian Earth Sci.*, **18**, 561–584.

Pognante, U., Castelli, D., Benna, P., Genovese, G., Oberli, F., Meier, M. & Tonarini, S. (1990) The crystalline units of the High Himalayas in the Lahul–Zanskar region (Northwest India); metamorphic-tectonic history and geochronology of the collided and imbricated Indian Plate. *Geol. Mag.*, **127**, 101–116.

Prell, W.L. & Kutzbach, J.E. (1992) Sensitivity of the Indian monsoon to forcing parameters and implications for its evolution. *Nature*, **360**, 647–652.

Quade, J., Cater, J.M.L., Ojha, T.P., Adam, J. & Harrison, T.M. (1995) Late Miocene environmental change in Nepal and the northern Indian subcontinent; stable isotopic evidence from Paleosols. *Geol. Soc. Am. Bull.*, **107**, 1381–1397.

Quade, J., Roe, J., DeCelles, P.G. & Ojha, T.P. (1997) The late Neogene $^{87}Sr/^{86}Sr$ record of lowland Himalayan rivers. *Science*, **276**, 1828–1831.

Ratschbacher, L., Frisch, W., Liu, G. & Chen, C. (1994) Distributed deformation in southern and western Tibet during and after India-Asia collision. *J. Geophys. Res.*, **99**, 19917–19945.

Raymo, M.E. & Ruddiman, W.F. (1992) Tectonic forcing of late Cenozoic climate. *Nature*, **359**, 117–122.

Richards, A., Argles, T.W.A., Harris, N.B.W., Parrish, R., Ahmad, T., Darbeyshire, F. & Draganits, E. (2005) Himalayan architecture constrained by isotopic tracers from clastic sediments. *Earth Planet. Sci. Lett.*, **236**, 773–796.

Robinson, D.M., DeCelles, P.G. & Copeland, P. (2006) Tectonic evolution of the Himalayan thrust belt in western Nepal: implications for channel flow models. *Geol. Soci. Amer. Bull.*, **118**; no. 7/8; p. 865–885; doi: 10.1130/B25911.1, 865–885.

Robinson, D.M., DeCelles, P.G., Garzione, C.N., Pearson, O.N., Harrison, T.M. & Catlos, E.J. (2003) Kinematic model for the Main Central Thrust in Nepal. *Geology*, **31**, 359–362.

Robinson, D.M., DeCelles, P.G., Patchett, P.J. & Garzione, C.N. (2001) The kinematic evolution of the Nepalese Himalaya interpreted from Nd isotopes. *Earth Planet. Sci. Lett.*, **192**, 507–521.

Sakai, H. (1983) Geology of the Tansen Group of the Lesser Himalaya in Nepal. *Mem. Fac. Sci. Kyushu Univ.*, **25**, 27–74.

Schelling, D. (1992) The tectonostratigraphy and structure of the eastern Nepal Himalaya. *Tectonics*, **11**, 925–943.

Schneider, C. & Masch, L. (1993) The metamorphism of the Tibetan series from the Manang area, Marsyandi Valley, central Nepal. In: *Himalayan tectonics* (Ed. by P.J. Treloar & M.P. Searle), *Geol. Soc. Lond.*, **74**, 357–374.

Searle, M.P. (1983) Stratigraphy, structure and evolution of the Tibetan-Tethys zone in Zanskar and the Indus suture zone in the Ladakh Himalaya. *Trans. Roy. Soc. Edinburgh: Earth Sci.*, **73**, 205–219.

Searle, M.P. (1991) *Geology and Tectonics of the Karakoram Mountains*. John Wiley and Sons, Chichester, p. 358.

Searle, M.P. & Godin, L. (2003) The South Tibetan detachment and the Manaslu Leucogranite; a structural reinterpretation and restoration of the Annapurna–Manaslu Himalaya, Nepal. *J. Geol.*, **111**, 505–523.

Searle, M.P., Simpson, R.L., Law, R.D., Parrish, R.R. & Waters, D.J. (2003) The structural geometry, metamorphic and magmatic evolution of the Everest Massif, High Himalaya of Nepal-South Tibet. *J. Geol. Soc. Lond.*, **160**, 345–366.

Searle, M.P., Waters, D.J., Stephenson, B.J., Kohn, M.J., Catlos, E.J., Ryerson, F.J. & Harrison, T.M. (2002) Pressure-temperature-time path discontinuity in the Main Central Thrust Zone, central Nepal; discussion and reply. *Geology*, **30**, 479–481.

Simpson, R.L., Parrish, R.R., Searle, M.P. & Waters, D.J. (2000) Two episodes of monazite crystallization during metamorphism and crustal melting in the Everest region of the Nepalese Himalaya. *Geology*, **28**, 403–406.

Srivastava, P. & Mitra, G. (1994) Thrust geometries and deep structure of the outer and lesser Himalaya, Kumaun and Garhwal (India): implications for evolution of the Himalayan fold-thrust belt. *Tectonics*, **13**, 89–109.

Stephenson, B.J., Searle, M.P., Waters, D.J. & Rex, D.C. (2000) Structure of the Main Central Thrust zone and extrusion of the High Himalayan deep crustal wedge, Kishtwar–Zanskar Himalaya. *J. Geol. Soc. Lond.*, **158**, 637–652.

Tapponnier, P., Arnaud, N., Wittlinger, G., Jingsui, Y., Zhigin, X., Roger, F. & Meyer, B. (2001) Oblique stepwise rise and growth of the Tibet plateau. *Science*, **294**, 1671–1677.

Thakur, V.C. (1998) Structure of the Chamba Nappe and position of the Main Central Thrust in Kashmir Himalaya. *J. Asian Earth Sci.*, **16**, 269–282.

Treloar, P.J. & Rex, D.C. (1990) Cooling and uplift histories of the crystalline thrust stack of the Indian Plate internal zones west of Nanga Parbat, Pakistan Himalaya. *Tectonophysics*, **180**, 323–349.

Upreti, B.N. & Le Fort, P. (1999) Lesser Himalayan crystalline nappes of Nepal; problems of their origin. In: *Himalaya and Tibet; Mountain roots to Mountain Tops* (Ed. by A. Macfarlane, R.B. Sorkhabi & J. Quade), *Geol. Soc. Am., Boulder*, **328**, 225–238.

Valdiya, K.S. (1980) *Geology of Kumaun Lesser Himalaya*. Institute of Himalayan Geology, Dehradun, p. 291.

Valdiya, K.S. (1995) Proterozoic sedimentation and Pan-African geodynamic development in the Himalaya. *Precam. Res.*, **74**, 35–55.

Vance, D., Bickle, M., Ivy-Ochs, S. & Kubik, P.W. (2003) Erosion and exhumation in the Himalaya from cosmogenic isotope inventories of river sediments. *Earth Planet. Sci. Lett.*, **206**, 273–288.

Vance, D. & Harris, N. (1999) Timing of prograde metamorphism in the Zanska Himalaya. *Geology*, **27**, 395–398.

Vannay, J.C. & Hodges, K.V. (1996) Tectonometamorphic evolution of the Himalayan metamorphic core between the Annapurna and Dhaulagiri, central Nepal. *J. Met. Geol.*, **14**, 635–656.

Villa, I.M. (1997) Direct determination of (super 39) Ar recoil distance. *Geochimica et Cosmochimica Acta*, **61**, 689–691.

Walker, J.D., Martin, M.W., Bowring, S.A., Searle, M.P., Waters, D.J. & Hodges, K.V. (1999) Metamorphism, melting, and extension; age constraints from the High Himalayan slab of Southeast Zanskar and Northwest Lahaul. *J. Geol.*, **107**, 473–495.

Weltje, G.J. (2002) Quantitative analysis of detrital modes; statistically rigorous confidence regions in ternary diagrams and their use in sedimentary petrology. *Earth Sci. Rev.*, **57**, 211–253.

White, N.M., Pringle, M., Garzanti, E., Bickle, M., Najman, Y., Chapman, H. & Friend, P. (2002) Constraints on the exhumation and erosion of the High Himalayan Slab, NW India, from foreland basin deposits. *Earth Planet. Sci. Lett.*, **195**, 29–44.

Willis, B. (1993) Evolution of Miocene fluvial systems in the Himalayan foredeep through a two kilometer-thick succession in northern Pakistan. *Sediment. Geol.*, **88**, 77–121.

Zuffa, G.G. (1985) *Provenance of Arenites*. D. Reidel Publishing Company, Dordrecht, p. 408.

Supplementary material

The following material is available for this article online at www.blackwell-synergy.com:

Data repository item S1 – Petrog & heavy min – post Tinau age conversion

Data repository item S2 – Whole rock Sr-Nd data

Data repository item S3 – All mica post Tinau age conversion

Please note: Blackwell Publishing are not responsible for the content or functionality of any supplementary materials supplied by the author. Any queries (other than missing material) should be directed to the corresponding author for the article.